Impact of land-use dynamics and climate change scenarios on Groundwater recharge in the case of Anger watershed, Ethiopia

Fikadu Warku Chuko [*], Abera Gonfa Abdissa

Department of Earth Sciences, Wollega University, P.O. Box 395, Nekemte, Ethiopia

ARTICLE INFO

ABSTRACT

An assessment of land use dynamics and climate variability impacts on hydrological processes is vital and a prerequisite for effective water resources management. This study aimed to quantify the effect of land-use changes and long-term climate variability on the Anger watershed's annual groundwater recharge, which covers a total drainage area of 7717 km^2. The WetSpass (Water and Energy Transfer between Soil, Plants, and Atmosphere under quasi-Steady State) model was used to investigate the impact of land cover and climate variability on groundwater. The Mann–Kendall (MK) test was used to analyze the spatial variations and temporal trends of the climate variables in the watershed. Input data for the model, such as land use, hydro-meteorological data, soil texture, topography, and groundwater elevation parameters, were prepared in the form of gridded maps with a 30 m resolution. The model results indicate that land-use change and climate variability considerably impact distributed groundwater recharges. Groundwater recharge decreased with land use in 2000 and 2019, respectively, as compared to baseline land usage (1985). The study also demonstrates how the anticipated future combination of less precipitation and higher temperatures has a detrimental effect on the watershed's annual average groundwater recharge. Future rising temperatures and reduced precipitation are projected to result in an average annual groundwater recharge showing significant decreases in 2050, 2080, and 2110, respectively, according to scenario-based models. The result has provided valuable information on the management and response of groundwater recharge to climate and land-use changes, particularly for the Anger watershed and for the total country as well.

1. Introduction

Groundwater is a finite and exposed resource that should be used efficiently and adequately for present and future generations [1]. Groundwater availability is directly dependent on precipitation recharge to the ground. Groundwater recharge links atmospheric, surface, and subsurface water components, and it's sensitive to climatic and land use/cover factors [2–4]. Besides, the spatial variation in groundwater recharge due to distributed land use, topography, soil type, slope, groundwater level, and meteorological conditions can be significant and accounted for [5,6]. Due to its significant change in temperature, precipitation, and potential evapotranspiration, climate affects the hydrological function and processes [7]. The significant changes in temperature and precipitation that occur nowadays are not only because of natural phenomena but also due to anthropogenic activities [8].

Groundwater recharging is significantly impacted by land use dynamics and climate changes [9]. According to Ref. [10], land use

---

changes are substantially higher now than it was in earlier decades. According to Ref. [11], between 2000 and 2020, agriculture expansion increased by 15% as a result of human activity, and by 2040, it was expected to have increased by 30%. According to Ref. [12], decreased groundwater recharge may be impacted by growing anthropogenic alteration and climate changes.

It has changed repeatedly throughout history, is changing now, and is probably going to change in the future. A significant effect of climate change is alterations in the evaporation, temperature, and precipitation characteristics that can affect runoff, frequency, and intensity of recharge and affect the availability of groundwater [13]. Climate change and human activity can have a significant impact on groundwater recharge [14]. The impact of land use and climate change on hydrological processes has been assessed over the past several decades, using (i) field-based data-driven statistical methods based on single catchments or paired catchments [15,16] and (ii) hydrological modeling [17–22]. Hydrological modeling using physically-based tools is widely used by water resource engineers and hydrologists in the investigation of hydrological systems [23].

As a result, it deteriorates natural resources, including water and resource aid related to water, which can negatively affect the environment and socio-economic well-being of the local community. Knowing the rate of land-use changes and their impacts on the hydrologic cycle is needed for the optimal management of natural resources and mitigation of resource degradation. To effectively manage groundwater resources in a watershed, land-use changes' historical and present impacts need to be assessed [24]. Understanding the time-series variation of the water resources, especially runoff, evapotranspiration, and recharge, is essential in the Anger watershed. Such time-series information will be critical for researchers, hydrologists, and policymakers to plan and make the right decisions timely.

An increase or decrease in certain land use classes, like agriculture intensification and decline of forest area, can alter groundwater recharge and other water balance components by affecting interception and infiltration processes [25,26]. The impacts of land-use
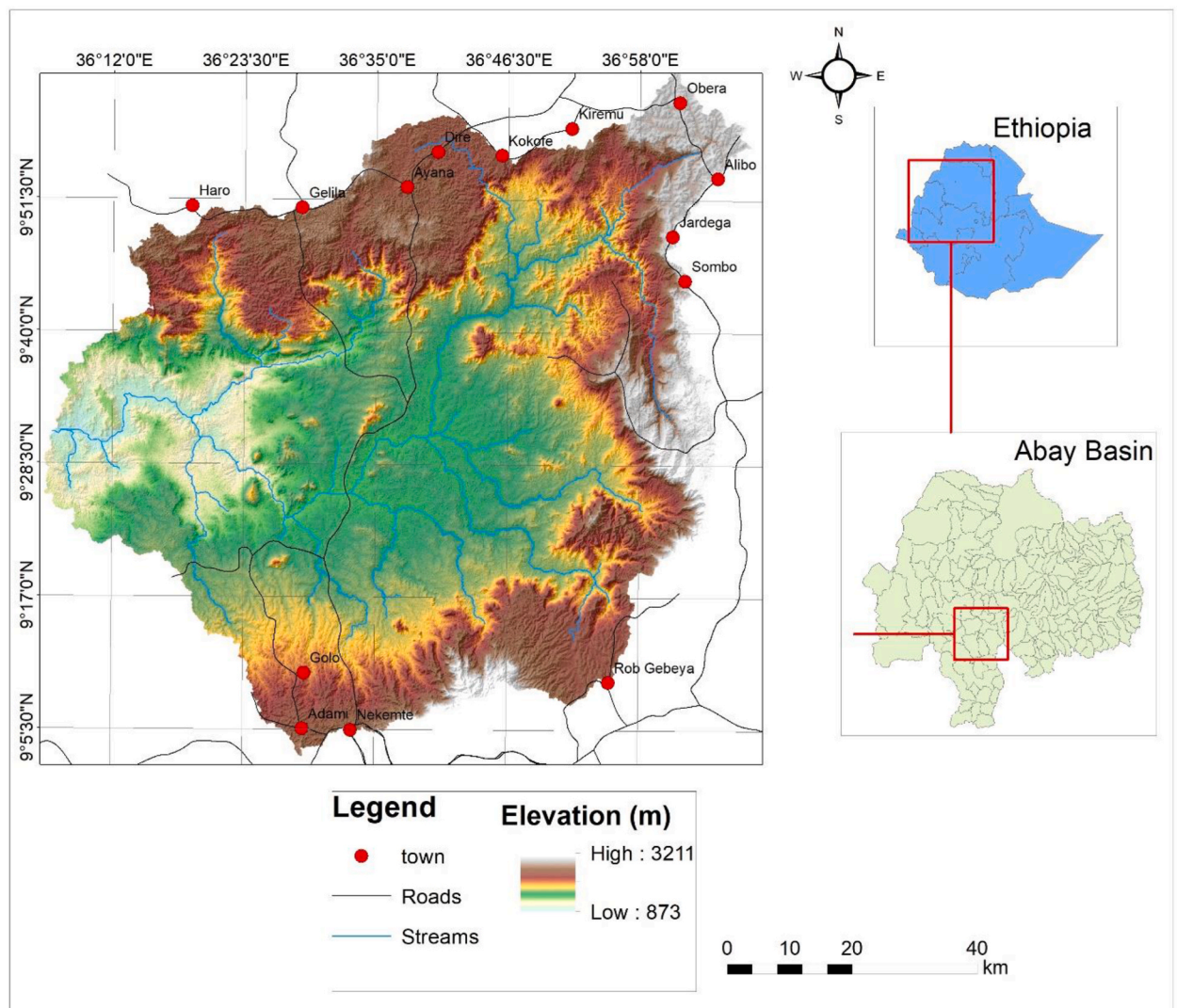

Fig. 1. Location map of Anger watershed.

change on the sustainability of ecosystems are becoming increasingly fundamental issues in global and local research. Ethiopia is part of a highly dynamic land-use change where more than 90% of the country's highlands were once forested in the past, and currently, the percentage of forest cover is less than 4% [27]. Deforestation, agricultural intensification, and urbanization are the prime causes of global and regional land-use changes.

However, the effect of land use and climate change on study watersheds in recent years on groundwater recharge is still not studied but is thought to be important for ensuring the sustainable management of the overexploited natural resource. Additionally, assessment by considering spatial, and long-term temporal land use and climate changes are vital for groundwater recharges to immediate intervention and future planning for the study area and the entire country as well.

Therefore, this study aims to assess the impact of land use and climate variability on groundwater recharge in the Anger Watershed using the WetSpass model. The specific objectives of this study are (i) to assess land-use changes; (ii) to analyze the trend of climate variability; and (iii) to simulate the impact of land dynamics and climate variability on distributed groundwater recharge in the Anger watershed.

2. Materials and methods

2.1. Study area

The study area is located in the Abay basin. Geographically, it is bounded between $9°\ 10'\ 0''$ to $10°0'\ 0''$ N Latitude and $36°\ 18'\ 0''$ to $37°\ 0'\ 0''$ E Longitude, and it has an elevation range from 873 m to 3211 m a.s.l. It covers a total drainage area of 7717 km^2 (Fig. 1). Natural resources such as forests and water in watersheds provide significant goods and services on which living organisms depend, such as provisioning, regulating, and supporting functions and services [28]. Land-use change can trigger resource degradation, affecting watershed properties and procedures that may affect groundwater resource availability [29].
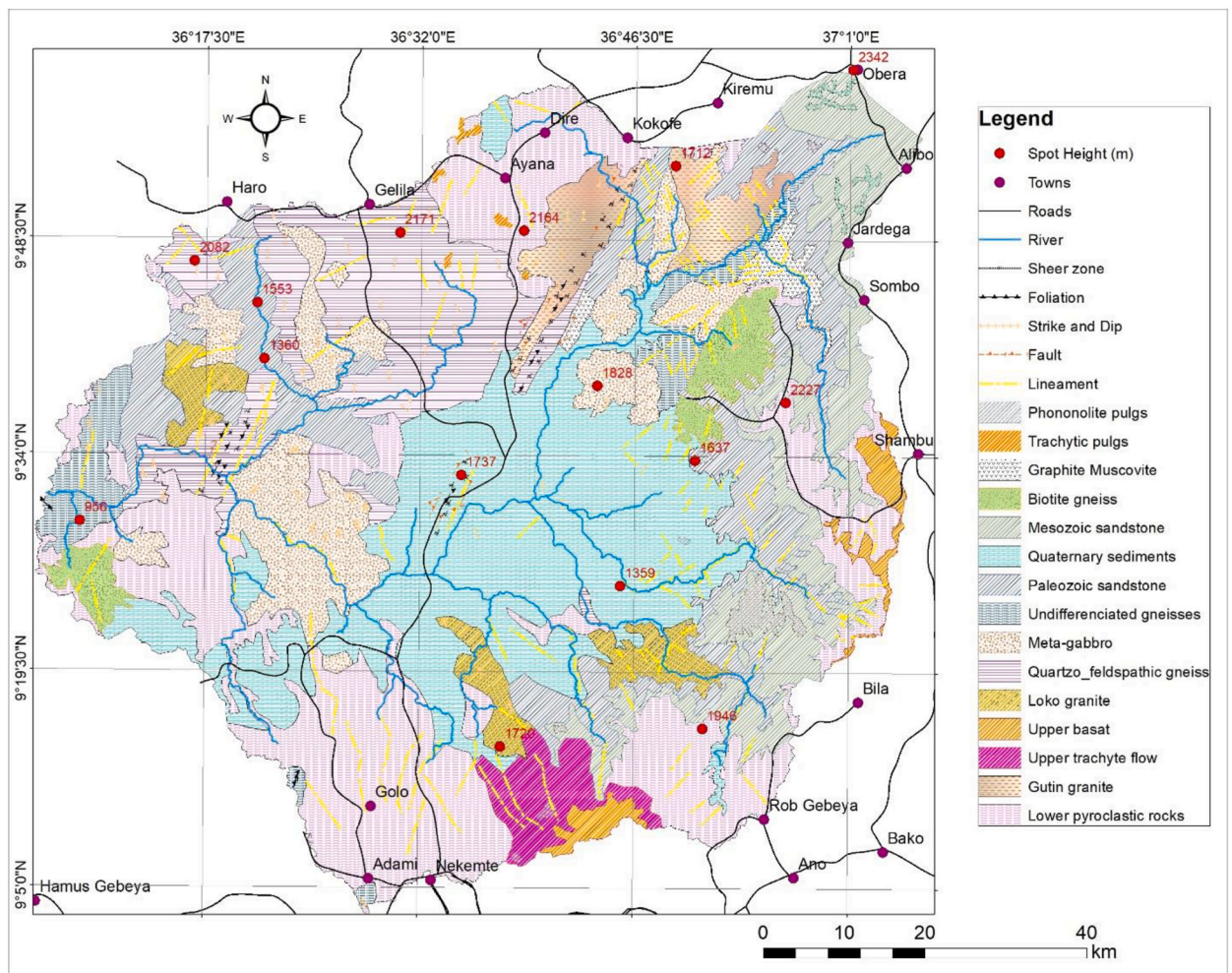

Fig. 2. Simplified Geologic map of the Anger watershed (adopted from GSE, 2000).

Deforestation, loss of biodiversity, habitat destruction, and a reduced ability of the watershed to sustain natural resources and ecosystem services are the consequences of land-use change [30,31]. In the watershed, the local community and investors engaged in extensive agricultural activities, resulting in lower infiltration rates and increased formation of surface runoff. These studies reflect efficient land use and climate change planning, which is a prerequisite for the effective management of groundwater resources in study watersheds.

2.2. Geological settings

According to [32], the central geologic units found in the study area include quaternary sediments, tertiary volcanic, Paleozoic and Mesozoic sedimentary rocks, and Precambrian metamorphic rocks. Quaternary sediments (black cotton soil, reddish, sandy soil, and alluvial soils) mainly cover the central part of the study area. Tertiary volcanics (upper basalt, lower basalt, upper trachyte flow, pyroclastic rocks, and lower pyroclastic rocks) mainly cover the southern and northern parts of the area. Paleozoic and Mesozoic sedimentary rocks include Mesozoic siltstone, Mesozoic sandstone, and Paleozoic sandstone. Precambrian intrusive and metamorphic rocks consist of mainly quartzo-feldspathic and undifferentiated gneisses, granite, and schists as shown in Fig. 2.

2.3. Data sources

The climate data used for driving the water balance were obtained from the Ethiopian National Meteorological Agency (NMA) for weather stations located within the watershed. In contrast, the potential evapotranspiration (PET) was calculated using the Hargreaves formula [33]. Minimum and maximum air-temperature data were used to compute potential evapotranspiration (PET). Landsat TM (1985, 2000) and OLI, 2020 were downloaded from USGS Earth Explorer to analyze land-use changes. A high-resolution (2020) Digital Elevation Model (DEM) (12.5 m × 12.5 m) data were downloaded from the Alaska Satellite Facility (ASF) (https://asf.alaska.edu/) to generate slope and topography data. The soil and streamflow data used for the study were obtained from the Ministry of Water and Energy of Ethiopia. The groundwater depth data was collected from the East Wollega zone Water, energy, and Mineral office.

2.4. Climatic characteristics

The study area is generally humid to sub-humid, with a mean annual rainfall of 1219–2090 mm y^{-1}. The maximum total annual rainfall in the watershed is 2090 mm at the Nekemte gauging station & the minimum full annual is 1219.1 mm at Ehud Gebeya station in the watershed (Fig. 3).

2.5. Climate trend analysis

Previous time-series studies of temperature and rainfall patterns in Ethiopia have been conducted at various spatial and temporal scales [34]. This study focused on the watershed-level analysis of precipitation, temperature, and PET to assess its impacts on groundwater recharge.

The long-term annual temperature and precipitation data (1985–2020) were analyzed to evaluate the temperature and precipitation change in the Anger watershed (Fig. 4). The Mann–Kendall trend test [35,36] and Sen's slope estimator were used to determining the trend in time series climatic variables data. The tests were carried out on annual rainfall, annual maximum and minimum temperature, annual average temperature, and potential evapotranspiration at 95% confidence levels. The Mann–Kendall trend test is
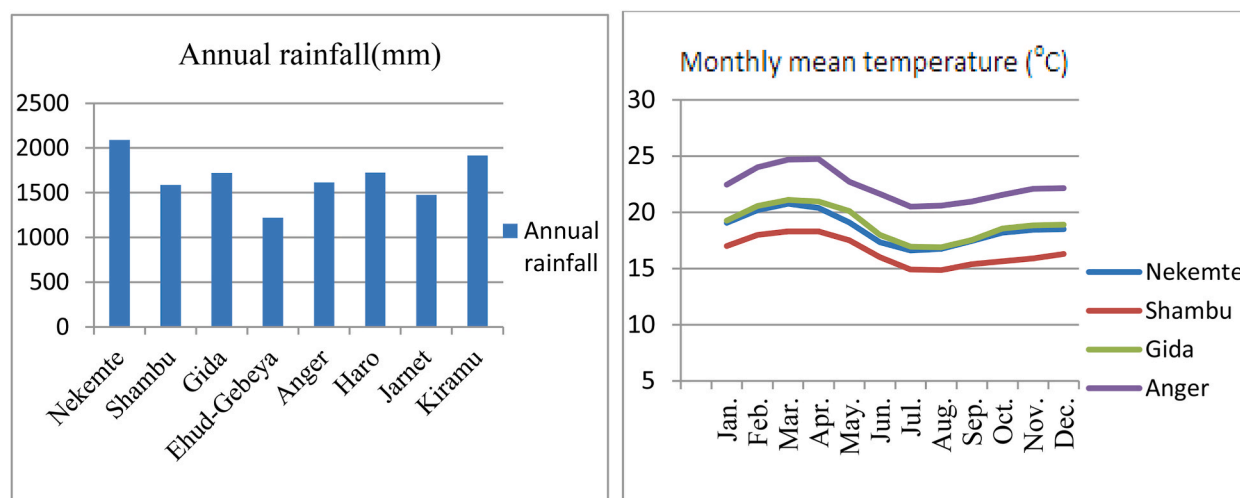

Fig. 3. Long-term average annual rainfall and long-term monthly mean temperature.
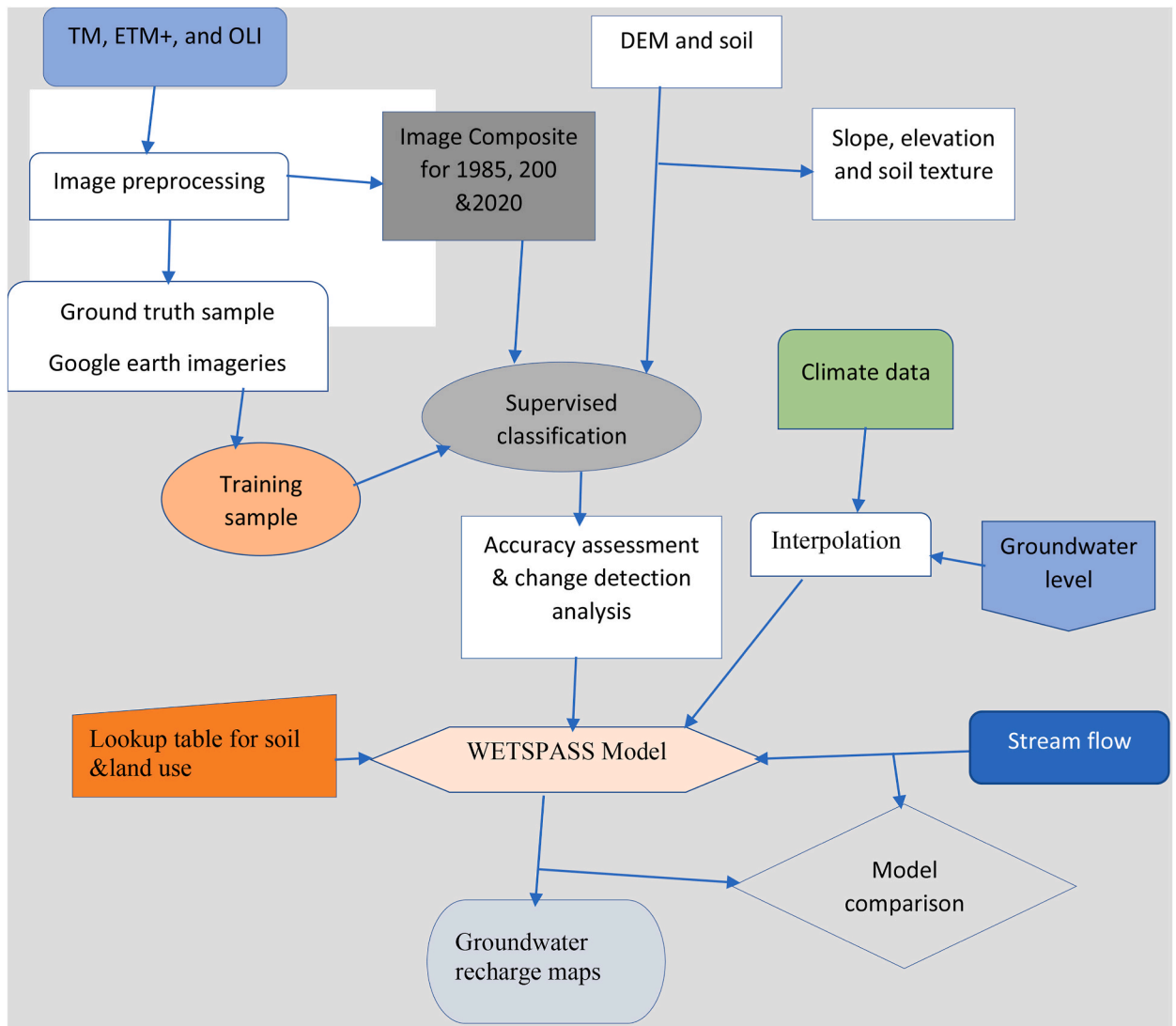
Fig. 4. Flow Diagram of WetSpass model.

the most widely used method for trend detection in hydro-climatic time series analysis [37–40], assumes a null hypothesis (Ho) that no trend is tested against the alternative hypothesis (H1) of the presence of a trend [41]. The mathematical equations (Equations (1)–(4)) for calculating Mann- Kendall Statistics S, VAR(S) and standardized test statistics Z are as follows:

For the time series $x_1,.., x_n$, the MK test statistic, S, is then computed as the sum of the number of positive differences minus the number of negative differences, or given by:

$$S = \sum_{i=1}^{n-1} \sum_{j=k=1}^{n} sgn(Xj - Xi) \tag{1}$$

where Xi and Xj are sequential environmental data, climate data, or hydrological data values for the time series data of length n, such that $(j > i)$ and where the sgn function is given as;

$$sgn(Xj - Xi) = \begin{cases} +1 \ if \ Xj > Xi \\ 0 \ \ if \ Xj = Xi \\ -1 \ if \ Xj < Xi \end{cases} \tag{2}$$

The variance of statistics is estimated as,

$$VAR(S) = \frac{N(N-1)(2n+5) - \sum_{j=1}^{m} Ui(i)(i-1)(2i+5)}{18} \tag{3}$$

where N is the length of the data set, Ui denotes the number of ties to an extent (sample) i.

$$Zs = \begin{cases} \dfrac{S-1}{\sqrt{VAR\,(S)}} & if\ S > 0 \\ 0 & if\ S = 0 \\ \dfrac{S+1}{\sqrt{VAR\,(S)}} & if\ S < 0 \end{cases}$$

(4)

The standard normal test statistic Zs (Equation (4)) indicates a trend in the data series with a positive or negative value, revealing increasing or decreasing trends, respectively. The R version 4.0.3 software was used to perform the statistical MK test analysis.

The Global Climate Models (GCMs; also known as General Circulation Models) projection and the hypothetical approach are two primary methods to generate future climate change scenarios for climate change impact assessment [42]. Global climate models (GCMs) are developed to simulate past climate and generate future modeled data on temperature, and precipitation, partially on the atmospheric concentration of greenhouse gases (GHGs) and other pollutants, derived from future scenarios and on the model simulation [43]. The hypothetical systems are purposively designed to represent changes in climate variables such as precipitation and temperature and, generally, consist of two steps [42,44].

Firstly, the average annual changes in precipitation and temperature for a fixed time slice are estimated (typically, let ΔT denote absolute change (°C) and ΔP relative change (%). Then, the historical temperature and precipitation series with the same length as the fixed time slice are perturbed by adding ΔT and multiplying (1 + ΔP), respectively [42,45].

Hypothetical climate change scenarios were formulated for three different times at a gap of 30-year intervals from a baseline starting from 2050, 2080, and 2110 to simulate the climate change scenario's impact on groundwater recharge. The model was computed by perturbing the meteorological input parameters (precipitation, temperature, and potential evapotranspiration) of the baseline WetSpass model. First, to select a reasonable range for the climate change scenarios, the variations of temperature and precipitation time series were analyzed using the MK trend test, as shown in Tables 4 and 5.

This was done by assigning percentage or value changes of climatic variables on an annual basis. Then, based on these scenarios and the present situation, annual recharge was simulated with the WetSpass model.

2.6. WetSpass Model set-up.

WetSpass (Water and Energy Transfer between Soil, Plants, and Atmosphere under a quasi-Steady State) was built upon the foundations of the time-dependent spatially distributed hydrological balance model "WetSpa" [5,46–48]. It is a physically-based, spatially distributed hydrologic model that considers the spatial variability of basin parameters, such as land cover, soil texture, topography, groundwater depth, and hydro-meteorological parameters for estimating groundwater recharge. The model calculates the long-term average, spatially varying, water-balance components: surface runoff, actual evapotranspiration, and groundwater recharge. The WetSpass model treats a basin or region as a regular pattern of raster cells. The total water balance for a raster cell is split into independent water balances for each cell's vegetated, bare-soil, open-water, and impervious parts. This subdivision allows one to account for the non-uniformity of the land use per cell, which depends on the raster cell's resolution [5]. The total water balance per raster cell is given as a summation of evaporation from bare soil and open water bodies, vegetation transpiration, and evaporation of precipitation intercepted by the vegetation (Equations (5- 7)).

$$ETraster = avETv + asEs + aoEo + aiEi$$ (5)

$$Sraster = avSv + asSs + aoSo + aiSi$$ (6)

$$Rraster = avRv + asRs + aoRo + aiRi$$ (7)

ETraster, Sraster, and Rraster represent the total evapotranspiration, surface runoff, and groundwater recharge of a raster cell. Each has a vegetated, bare-soil, open-water impervious area component denoted by a_v, a_s, a_o, and a_i, respectively.

Geographic Information Systems software (ArcGIS) was used to prepare WetSpass input data for the model, with a cell size of 30 m and 30 m. The spatial input data necessary for running the model include grids of land use, soil, topography (m), Slope (%), Groundwater depth (m), precipitation (mm y^{-1}), potential evapotranspiration (mm y^{-1}), air temperature (°C), Wind speed (m s^{-1}). The land use and soil parameters are linked to the model by attribute tables [49]. Attribute tables contain the soil parameter, runoff coefficient, and land-use parameter. The time series of PET data was calculated using the Hargreaves equation [50] (Equation (8)).

$$PET = 0.0023(T_{mean} + 17.8)(T_{max} - T_{min}) \times 0.5Ra$$ (8)

where PET is the potential evapotranspiration (mm/day); Tmean, Tmax, and Tmin are average, maximum, and minimum temperature (°C) values, respectively; Ra is extra-terrestrial radiation (mm day^{-1}). The model was run using the three different years' land-use maps (1985, 2000, and 2020) to simulate the impact of land-use change on groundwater recharge of the catchments while keeping the meteorological data and other parameters constant.

2.6. Base flow separation

Simulated groundwater recharge was compared against the estimated base flow. Numerous analytical methods have been developed for baseflow separation from total stream flow [51–53] In this study, WHAT (Web-based Hydrograph Analysis Tool) [52] was used for baseflow separation, providing three techniques for baseflow separation; Local Minimum Method, One Parameter Digital Filter, and Recursive Digital Filter. The digital filter method has been used in base flow separation to identify the high-frequency signal from the low-frequency signal [54] because high-frequency waves correspond to direct runoff, and low-frequency waves can be associated with the base flow [55].

The general form of the Eckhardt Recursive Digital Filter method (Equation (9)) considering a digital filter parameter [55] is:

$$bt = \frac{(1 - \text{BFImax}) * \alpha + bt - 1 + (1 - \alpha) * \text{BFImax} * Qt}{1 - \alpha * \text{BFImax}} \tag{9}$$

where bt is the filtered base flow at the t (m/s), bt-1 is the filtered base flow at the t−1 time step (m/s), BFImax is the maximum value of the base flow index (BFI), which is the maximum values of the long-term ratio of base flow to total streamflow; α is the filter constant, and Qt is the total streamflow at the t time step ($m^3 s^{-1}$).

Representative BFImax values were estimated for different hydrological and hydrogeological situations by comparing the results from conventional separation techniques with the digital filter method to reduce the subjective influence of using BFImax on baseflow separation [55]. Therefore, [55] gives estimates for the use of BFImax values based on the type of streamflow and aquifer: 0.80 for
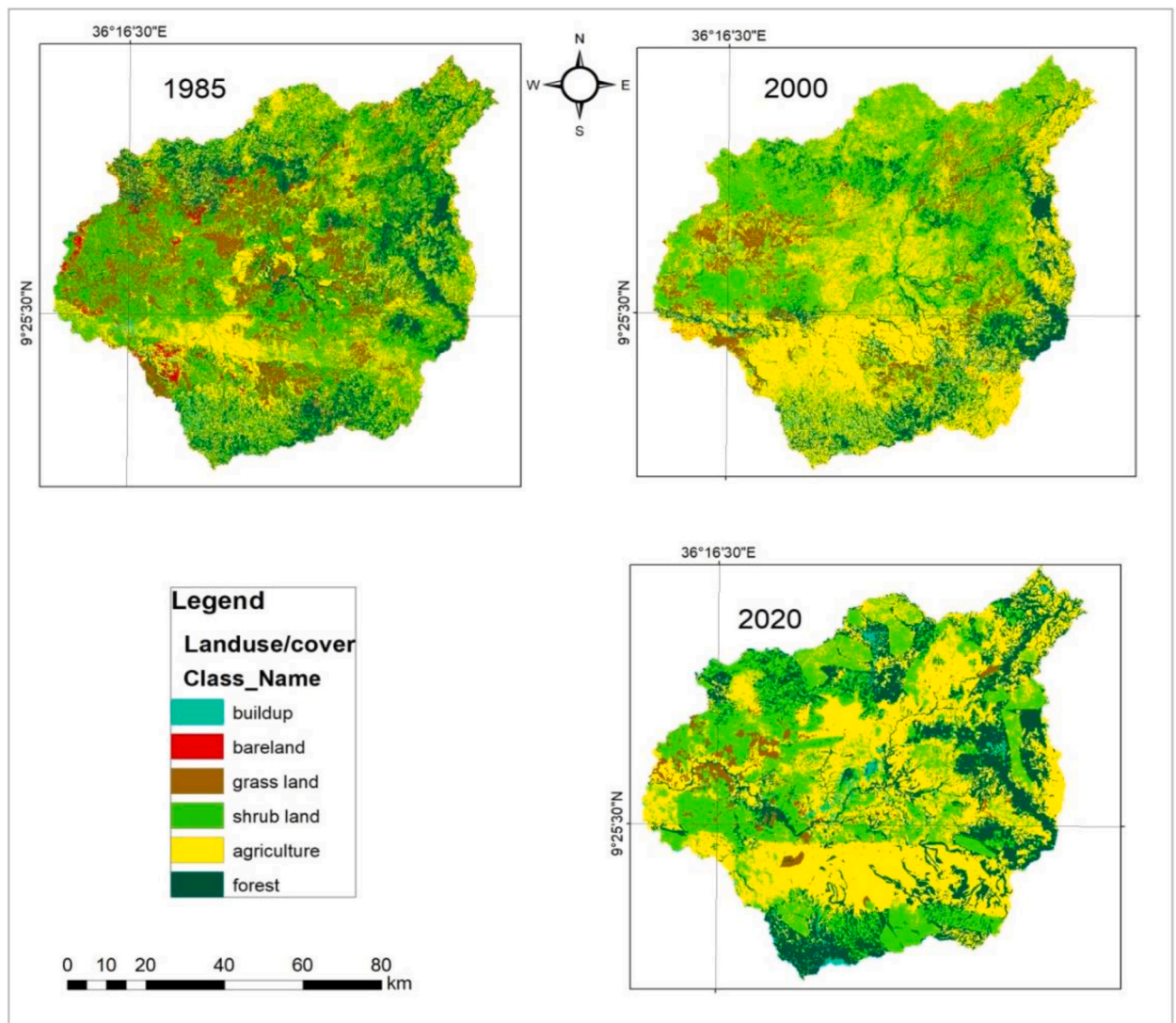

Fig. 5. Land use maps of 1985, 2000 and 2020.

perennial streams with porous aquifers; 0.50 for ephemeral streams with porous aquifers; and 0.25 for perennial streams with hard rock.

3. Result

Verification of the accuracy of the results for the classed maps was done by accuracy evaluation. Each class provided about 20 observations, which were used to evaluate the correctness of the results. Data from 1985 had an overall accuracy of 79%, 86% in 2000, and 90% in 2020 respectively. The kappa coefficient was 0.78 in 1985, 0.87 in 2017, and 0.91 in 2020. Finally, a post-classification approach was used to display the findings of the change detection, and the dynamic land-use change detection matrix between three land-use states was computed (Fig. 5 and Table 1).

3.1. Land use and land cover change analysis

The change detection matrix was computed for each phase and change for the entire 35-year period and identified what was changed. The statistical change detection matrix report tables for each class were calculated using ERDAS 2015. Tables 2 and 3 show the land-use change from one class to another in a hectare from 1985 to 2000 and 2000 to 2020, respectively.

Between 1985 and 2000, 22% of the Grassland land-use types remained as grassland, where 23% was converted to agriculture, 32% to shrubland, and 16% to forest. On the other hand, 32% of classes of agriculture were unchanged, where 33% were to shrubland, 9% to the forest, and 20% to grassland. For forest, 47% stayed the forest, where 1% to buildup, 8.8% shrubland, and 11.5% agriculture. From the shrubland class, 24.7% converted to agriculture, 19.7% to the forest, and 40% remained the same (Table 2).

Between 2000 and 2020, one class areas were partially converted to other classes and vice versa. Accordingly, Shrubland's 57% class was unchanged in 2020 where 3.7% to buildup, 23.5% to agriculture, 11% to the forest, and 3% to grassland. The agriculture 36% unconverted class in 2020 where 3% converted to buildup, 45% to shrubland, and 9% to forest. The forest class of 28% remains the same in 2020 where 1.6% to buildup, 51.5% shrubland, 14% agriculture, and 3% grassland. From the grassland class, 8% converted to buildup, 38% to shrubland, 36% to agriculture, and 7% to the forest, where 6% ha remain the same (Table 3).

3.2. Climate change and trend analysis

The obtained statistical results from Mann-Kendall trend tests and Sen's Slope are presented in Table 4. The tests were carried out on annual rainfall, annual maximum and minimum temperature, annual average temperature, and potential evapotranspiration.

3.3. Recharge under different land use/land cover

The long-term average annual recharge obtained from the WetSpass model for the whole Anger Watershed under land use of 1985, 2000, and 2020 is 233.86 mm (14.74%), 224.40 mm (14.17%), 208.26 mm (13.12%) respectively. The result shows that land use significantly affects the groundwater recharge of the study watershed (Fig. 6).

3.4. Groundwater recharge under different climate scenarios

Since the twentieth century, climate change has become the world's most concerning environmental issue. The consequences of global climate pose a critical threat to ecological, biophysical, and socio-economic aspects and have reached an alarming state [56].

According to the Intergovernmental Panel on Climate Change [57], the global temperature has increased by 0.6 ± 0.2 °C since 1861 and is expected to increase by 2–4 °C over the next 100 years. Recharge responds strongly to the temporal pattern of precipitation as well as soil cover and soil properties [58]. Temperature changes also affect the hydrologic processes by directly changing the evaporation of available surface water and vegetation transpiration. In addition, these changes can influence the amounts of rainfall, duration, and intensity and thus indirectly affect surface and subsurface water storage and flux [59].

Only two of the nine precipitation stations in and around the study area show an increasing trend, while the other seven show a decreasing trend. Similarly, the temperature data analysis of four stations indicates that three (Nekemte, Shambu, and Gida) show a

Table 1
Land use changes from 1985 to 2020.

Land use/cover Class	1985		2000		2020	
	Km^2	%	Km^2	%	Km^2	%
Agriculture area	1915.57	24.8	3310.5	42.85	3915	50.68
Build up area	90	1.16	178.5	2.3	254	3.28
Shrub land	2834.88	36.7	2400	31.07	2086	27
Grassland	1049	13.58	615	7.96	388	5.02
Bare land	266.84	3.45	39	0.50	29	0.37
Forest	1567.77	20.29	1180.8	15.28	1052	13.61
Total	**7724**	**99.98**	**7724**	**99.97**	**7724**	**99.97**

Table 2

Change detection matrix from 1985 to 2000.

the year 1985								
the year 2000		Grassland	agriculture	Build up	Bare land	shrubland	Forest	Class Total
	Grassland	6166.5	6577	654.7	1365	9072	4507	28342.3
	agriculture	42307	68105	3065	7591	70385.8	19172.6	210626.4
	Build up	5909	6045.7	701	660	9119.7	1236	23671.4
	Bare land	1030	2075	234	897	2210	1122	7568
	shrubland	40910	96033	3945.9	15491	155583	76410	388372.9
	Forest	8801	13112	1098.7	1608.8	35272	53969	113861.5
	Total	105123.5	191947.7	9699.3	27612.8	281642.5	156416.6	772442.3

Table 3

Change detection matrix from 2000 to 2020.

	The year 2000						
the year 2020		shrubland	Bareland	grassland	buildup	Forest	agriculture	Class Total
	shrubland	119288	2482	6774.7	7629	23240	49030.7	208444.4
	Bare land	1745	51.9	48	101.9	269	712.9	2928.67
	Grassland	7551.5	200.9	1043	1714.5	1378	6932	18819.8
	Build up	7248	147	470	726.7	1516.9	5358	15466.6
	Forest	100459	1294.9	7243	3104	55495.8	27464	195060.7
	agriculture	151974	3390	12752	10388	31929.7	121057	331490.7
	Class Total	388265.5	7566.7	28330.7	23663	113829	210554.6	772210.9

Table 4

MK and Sen's slope results for the annual time series (rainfall, maximum temperature, minimum temperature, average temperature, and PET).

Stations	S	VAR(S)	Z	Sen's Slope	p-value	Signific.	tau
Rainfall							
Anger	2.000	2842.000	0.019	0.105	0.985		0.005
Gida	−31.000	2058.330	−0.661	−4.181	0.509		−0.095
Nekemte	50.000	2842.000	0.919	5.754	0.358		0.123
Shambu	−106.000	2842.000	−1.970	−10.220	0.049	*	−0.261
Ehud Gebeya	−2.000	950.000	−0.032	−0.026	0.974		−0.011
Jarnet	−21.000	1433.670	−0.528	−3.927	0.597		−0.083
Haro	−37.000	817.000	−1.260	−8.429	0.208		−0.216
Kiramu	−7.000	697.000	−0.227	−5.600	0.820		−0.046
Maximum temperature							
Anger	68.000	950.000	−2.174	−0.080	0.030	*	−0.358
Gida	113.000	1257.660	3.158	0.062	0.002	**	0.489
Nekemte	177.000	3141.660	3.140	0.030	0.002	**	0.407
Shambu	159.000	2058.330	3.483	0.060	0.0004	**	0.489
Minimum temperature							
Anger	−26.000	950.000	−0.811	−0.021	0.417		−0.137
Gida	114.000	1096.660	3.412	0.065	0.0006		0.543
Nekemte	206.000	2842.000	3.845	0.035	0.0001	**	0.507
Shambu	134.000	1833.330	3.106	0.070	0.002	**	0.447
Average temperature							
Anger	56.000	950.000	−1.784	−0.040	0.074		−0.295
Gida	110.000	1096.660	3.292	0.064	0.0009	**	0.524
Nekemte	232.000	2842.000	4.333	0.041	0.00001	***	0.571
Shambu	176.000	1833.330	4.087	0.083	0.00004	***	0.587
PET							
Anger	−56.000	950.000	−1.784	−5.454	0.074		−0.295
Gida	16.000	1096.67	0.453	0.646	0.651		0.076
Nekemte	85.000	3141.670	1.499	1.038	0.134		0.195
Shambu	−20.000	1833.330	−0.444	−2.068	0.657		−0.067

*, ** and *, **, and *** represent variables of significance (* <0.05, ** <0.01, *** <0.001). A positive (+) value represents an increasing (upward) trend and a negative (−) represents a decreasing (downward) trend over time. The trends in the annual mean at six stations (Shambu, Gida, Ehud Gebeya, Jarnet, Kiramu, and Haro) revealed that precipitation is decreasing. Except for Shambu station, annual precipitation shows a non-significantly decreasing trend. On the other side, Anger and Nekemte stations show a non-significant (p > 0.05) increasing trend. The annual average temperature of three stations (Nekemte, Gida, and Shambu) indicates statistically significant increasing trends (p < 0.05), while the Anger station shows a non-significant (p > 0.05) increasing trend. The time series potential evapotranspiration was estimated for four stations (i.e., Arger, Gida, Nekemte, and Shambu). Only these stations have time-series temperature data to calculate potential evapotranspiration. There was no statistically significant increasing or decreasing trend in the average annual potential evapotranspiration for all stations (Anger, Gida, Nekemte, and Shambu) during the study period.

Table 5
Formulated hypothetical climate scenarios.

| station	X	Y	baseline rainfall (long-term average)	Rate (change/year)	2050	2080	2110
Nekemte	36.46	9.08	2089.97	5.75	2262.47	2434.97	2607.47
Shambu	37.12	9.57	1587.50	−10.22	1280.90	974.30	667.70
Gida	36.62	9.87	1719.75	−4.2	1593.75	1467.75	1341.75
Ehud Gebeya	36.43	9.22	1219.07	−0.03	1218.17	1217.27	1216.37
Anger	36.33	9.27	1615.81	0.11	1619.11	1622.41	1625.71
Haro	36.45	9.90	1722.82	−8.43	1469.92	1217.02	964.12
Jarnet	37.02	9.80	1474.88	−3.93	1356.98	1239.08	1121.18
Kiramu	36.80	9.92	1917.11	−5.6	1749.11	1581.11	1413.10
Station	**X**	**Y**	**baseline temperature (^{0}C)**	**Rate (change/year)**	**2050**	**2080**	**2110**
Nekemte	36.46	9.08	18.57	0.041	19.80	21.03	22.26
Shambu	37.12	9.57	16.51	0.083	19.00	21.49	23.98
Gida	36.62	9.87	18.97	0.064	20.89	22.81	24.73
Anger	36.33	9.27	22.34	−0.04	21.14	19.94	18.74
Stations	**X**	**Y**	**baseline PET**	**Rate (change/year)**	**2050**	**2080**	**2110**
Gida	36.62	9.87	1439.77	0.65	1459.27	1478.76	1498.26
Nekemte	36.46	9.083	1494.30	1.04	1525.50	1556.70	1587.90
Shambu	37.12	9.57	1432.38	−2.07	1370.28	1308.18	1246.08
Anger	36.64	9.57	1800.13	−5.45	1636.63	1473.13	1309.63
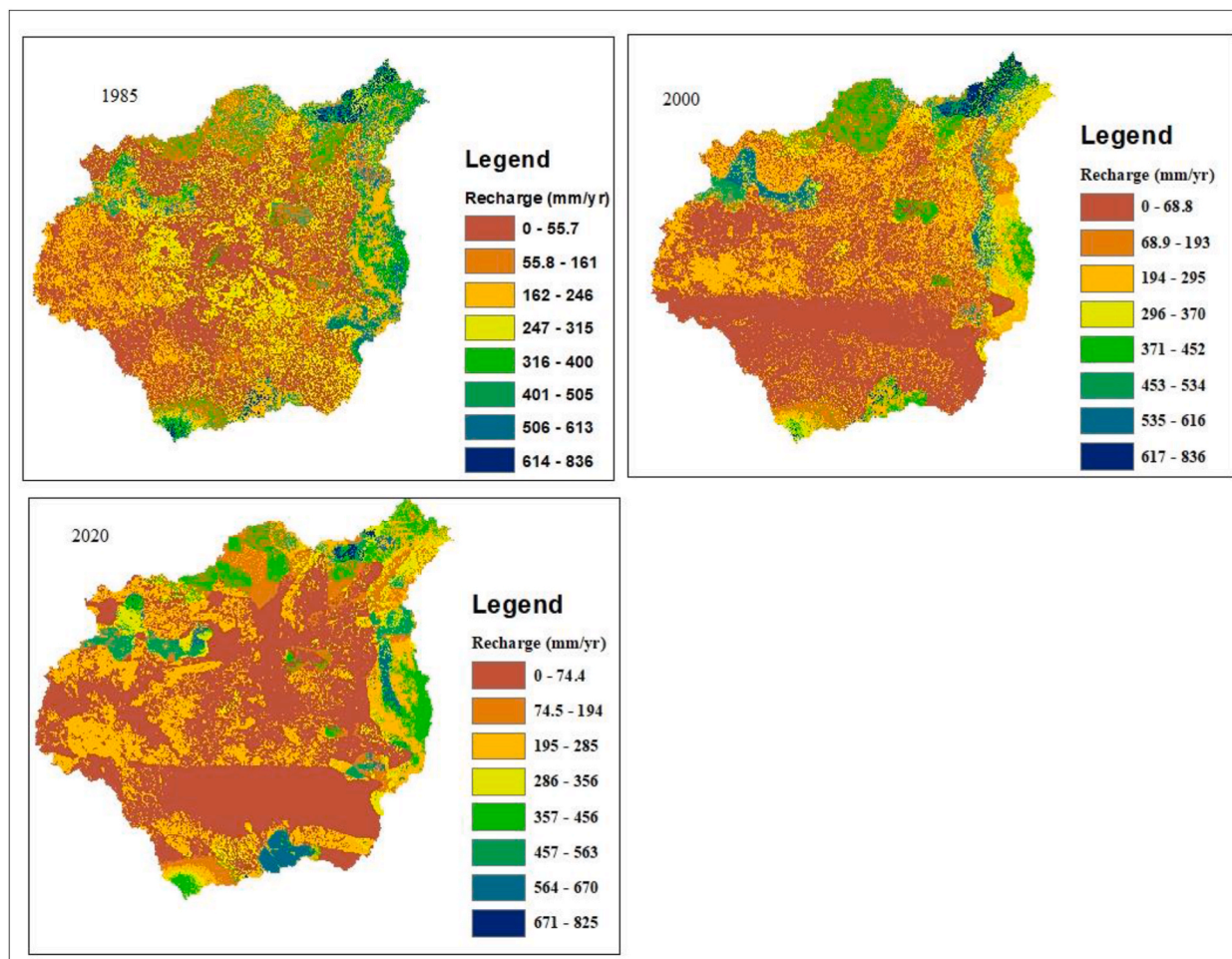
Fig. 6. Spatial variation of simulated long-term average annual recharge under different land-use scenarios (1985, 2000, and 2020). The classification is based on Natural Breaks (Jenks).

significant increasing trend, and the Anger station shows an insignificant decreasing trend. Sen's slope determined the magnitude of change per year (Table 4). We prepared hypothetical climate change scenarios and assessed their impact on groundwater recharge based on the change. This is done by assigning percentage or value changes of climatic variables on an annual basis, as shown in Table 5. Based on these scenarios, annual recharge was simulated by the WetSpass model (Fig. 7).

Based on the formulated hypothetical climate scenarios (Table 5), the average groundwater recharges of 2050, 2080, and 2110 will be 213.18 mm, 202.11 mm, and 198.36 mm, respectively. The modeling presented here demonstrates that the annual groundwater recharges are predicted to decrease compared to the baseline.

3.5. Model comparison

The simulated groundwater recharge values, by using WetSpass, were compared against observations of river flow at the Anger River gauge station, which accounts for about 60% of the study area (4515 km^2). Simulated groundwater recharges are compared against the estimated base flow as given in Table 4.

The study area is characterized by different geologic units: quaternary sediments, tertiary volcanic, Paleozoic and Mesozoic sedimentary rocks, and Precambrian metamorphic rocks including the gauged catchment. Hence, the aquifer is both a porous and hard rock aquifer with perennial streams. Therefore, the average base flow of porous and hard rock aquifers was considered the mean annual base flow during flow separation.

The difference between the simulated and observed groundwater recharge from the base flow is 68.7 mm. The mean annual simulated recharge is 244.33 mm (15.51%), and the mean observed yearly recharge from the base flow is 306.2 mm (19.31%).

4. Discussion

4.1. Impact of land-use change on groundwater recharge

Land-use change detection indicated that the agricultural area increased by 25.88%, while the shrubland and forest decreased by 9.7% and 7%, respectively. The results showed a significant land-use change in agricultural land during the study period. This is due to the rapid population increase; agriculture-based economies and a lack of institutional and policy-based land use management are the major driving forces for the study of watershed changes in land use.

The catchment's estimated annual recharge rates vary widely among and within land-use/land-cover settings (Fig. 6). In general, compared to the baseline conditions (1985), simulations under land use of 2000 and 2020 indicated a decrease in the mean annual groundwater recharge by 4.05% and 10.95% respectively. Therefore, converting natural land cover (forest, shrubland, and grasslands) to agricultural land increases surface runoff and decreases groundwater recharge of the catchment.

Other similar studies in Ethiopia found that increasing agricultural land and diminishing natural land cover increased runoff, decreasing recharge [29,60–64] and, [65]. Consequently, intensive agricultural activities that remove vegetation cover expose dense soils to erosion, reducing groundwater recharge. Groundwater recharge is impacted by changes in land use by altering the composition of the water balance [66,67]. Changes in land use caused by humans during the past few decades have impacted hydrological elements including recharging and runoff [68]. The development of phenomena like agricultural expansion, urbanization, desertification, and the disappearance of forests, is the main cause of the groundwater recharge changes [69].

4.2. Impact of climate change on groundwater recharge

Regarding temperature (minimum, maximum, and mean monthly temperature) during study periods, three stations (Gida, Nekemte, and Shambu) showed an increasing trend, and the Anger station showed a decreasing trend. Similarly, the previous study conducted by Ref. [70] reported future minimum and maximum increases over the Didessa basin, in which our study catchment is included. The study reported that the average monthly maximum temperature increase ranges from +0.40 °C to +1.86 °C by 2030s. There is consistency with our study, as most stations show an increasing trend. The annual potential evapotranspiration of the study area indicates an increasing trend. The increase in temperature will be followed by a likely increase in the annual evapotranspiration of the study area. A study by Ref. [71] reported that the Upper Blue Nile annual rainfall amount will change by −2.8 to 2.7%, with a likely increase in annual potential evapotranspiration (in 2041–2070). Our result, despite study area coverage, is more consistent with the report of the study.

Climate change represents long-term changes in meteorological parameters, such as temperature and precipitations and changes in these parameters affect groundwater recharge, storage, and levels, [72]. On the other hand, a considerable decrease in groundwater storage may likely lead to changes in other hydrological variables, such as baseflow reduction [73]. According to the findings of this study, climate change has a significant impact on groundwater recharge in the studied watershed. The predicted decline in recharge rates will be linked to lower mean annual rainfall and a rise in air temperature and evapotranspiration. Consequently, other hydrological elements of the watershed may be considerably impacted by a decline in groundwater recharge. For instance, according to Ref. [74] the future stream flow of the Anger River showed a decrease in the 2080s (2080–2100). It can therefore be assumed that the decline in stream flow of the Anger River might arise from a decrease in groundwater discharge to the stream and precipitation. As a result, total water yields in the watershed may be decreased in the future.
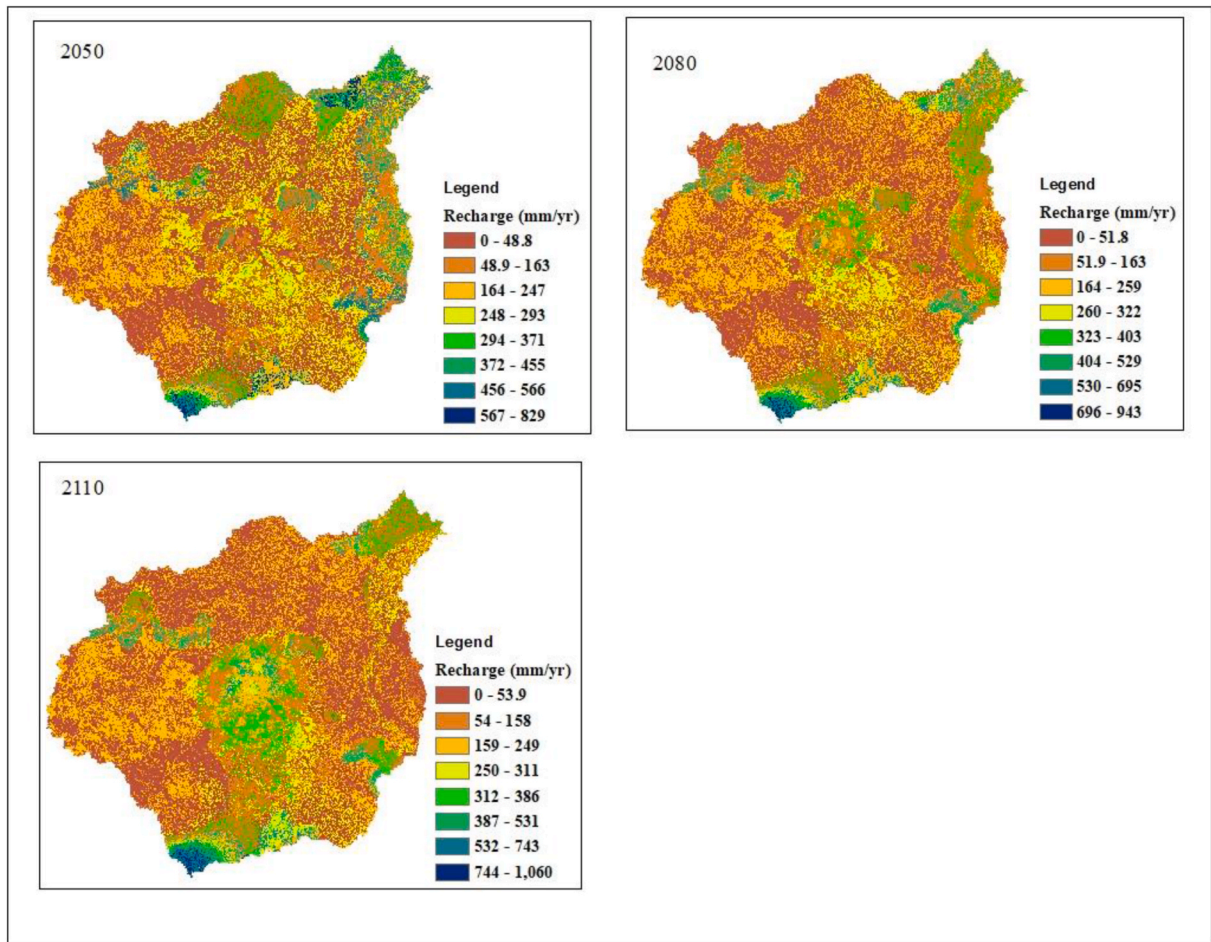
Fig. 7. Hypothetical scenarios of future groundwater recharge (2050, 2080, and 2110).

4.3. Study limitation and uncertainty

Despite these promising results, the study is limited to current and historical land use and land cover. This study would not take into account future land use and land cover. On the other hand, there are many possible sources of uncertainty in climate and hydrological models. The sources of model uncertainties could be input variables (e.g., hydroclimatic data, soil, land use) and model parameters. As a result, the study's findings should be carefully evaluated and can be considered representative of the likely future rather than accurate predictions.

5. Conclusion

In this study, the distribution of groundwater recharge in the Anger watershed is characterized by land use dynamics and climatic changes. There have been significant alterations in land use and climate over the past 34 years, according to an analysis of long-term changes in the study watershed. Runoff volume and percolation rate increased as a result of agricultural intensification and forest degradation, respectively. Parallel, to this, the study found that rising temperatures and a decline in rainfall rates were responsible for the study watershed's declining recharge. Land use dynamics and climate changes within a watershed preen the groundwater recharge. This study demonstrated how the natural resources of the Anger watershed are being significantly altered. Thus, to prevent future resource depletion, it is important to monitor the extent of resource alteration in the study watershed and its effects on water and other resources. This could provide information for smart resource management based on a sense of responsibility for future land use planning. Accordingly, for the study watershed and other similar watersheds, comprehensive watershed management is necessary to mitigate the detrimental effects of these changes on the ecosystem and groundwater recharge. For the study of watersheds, integrated natural resource management is needed to address human needs and optimize ecological function through upstream and downstream, wide-ranging, multi-stakeholder-driven activities. The findings of this study are convenient to other watersheds that share related biophysical and socio-economic appearances with the Anger watershed.

Author contribution statement

Fikadu Warku Chuko: Conceived and designed the experiments; Performed the experiments; Analyzed and interpreted the data; Contributed reagents, materials, analysis tools or data; Wrote the paper.

Abera Gonfa Abdissa: Analyzed and interpreted the data; Contributed reagents, materials, analysis tools or data; Wrote the paper.

Data availability statement

Data will be made available on request.

Declaration of competing interest

The authors declare no conflicts of interest.

Acknowledgments

References

[1] B. Arkoprovo, J. Adarsa, M. Animesh, Application of remote sensing , GIS and MIF technique for elucidation of groundwater potential zones from a part of Orissa coastal tract, Eastern India 2 (11) (2013) 42–49.

[2] M.I. Jyrkama, J.F. Sykes, The impact of climate change on spatially varying groundwater recharge in the grand river watershed (Ontario), J. Hydrol. 338 (3–4) (2007) 237–250, https://doi.org/10.1016/j.jhydrol.2007.02.036.

[3] M. Herrera-Pantoja, K.M. Hiscock, The effects of climate change on potential groundwater recharge in Great Britain, Hydrol. Process. 22 (1) (2008) 73–86, https://doi.org/10.1002/hyp.6620.

[4] J. P. B, A.T.W.1I.P. Holman1, M. Rivas-Casado1, N.J.K. Howden1, Natural Resources Department, Cranfield University, Cranfield, UK British Geological Survey, 2008, Wallingford, UK," no, 2009.

[5] O. Batelaan, F. De Smedt, WetSpass: A Flexible, GIS Based, Distributed Recharge Methodology for Regional Groundwater Modelling vol. 269, IAHS-AISH Publ, 2001, pp. 11–18.

[6] W. Dragoni, B.S. Sukhija, Climate change and groundwater : a short review, January 2009, Geol. Soc. Spec. Publ. 288 (2008) 1–12, https://doi.org/10.1144/SP288.1.

[7] A. Syed, et al., Assessment of climate variability among seasonal trends using in situ measurements: a case study of Punjab, Pakistan, Atmosphere 12 (8) (2021) 939, https://doi.org/10.3390/atmos12080939.

[8] H. Tabari, S. Marofi, Changes of Pan evaporation in the west of Iran, Water Resour. Manag. 25 (1) (2011) 97–111, https://doi.org/10.1007/s11269-010-9689-6.

[9] U. Ghimire, S. Shrestha, S. Neupane, S. Mohanasundaram, O. Lorphensri, Climate and land-use change impacts on spatiotemporal variations in groundwater recharge: a case study of the Bangkok Area, Thailand, Sci. Total Environ. 792 (2021), 148370, https://doi.org/10.1016/j.scitotenv.2021.148370.

[10] G. Shi, N. Jiang, L. Yao, Land use and cover change during the rapid economic growth period from 1990 to 2010: a case study of Shanghai, Sustain. Times 10 (2) (2018), https://doi.org/10.3390/su10020426.

[11] N.N. Dey, A. Al Rakib, A. Al Kafy, V. Raikwar, Geospatial modelling of changes in land use/land cover dynamics using Multi-layer perception Markov chain model in Rajshahi City, Bangladesh, Environ. Challenges 4 (May) (2021), 100148, https://doi.org/10.1016/j.envc.2021.100148.

[12] M.A. Mojid, M. Mainuddin, Water-saving agricultural technologies: regional hydrology outcomes and knowledge gaps in the eastern gangetic plains-a review, Water (Switzerland) 13 (2021) 5, https://doi.org/10.3390/w13050636.

[13] S. Kidanemariam, H. Goitom, Y. Desta, Coupled application of R and WetSpa models for assessment of climate change impact on streamflow of Werie Catchment, Tigray, Ethiopia, J. Water Clim. Chang. 12 (3) (2021) 916–936, https://doi.org/10.2166/wcc.2020.238.

[14] W. Wang, et al., Response of the groundwater system in the Guanzhong Basin (central China) to climate change and human activities, Hydrogeol. J. 26 (5) (2018) 1429–1441, https://doi.org/10.1007/s10040-018-1757-7.

[15] A.E. Brown, L. Zhang, T.A. McMahon, A.W. Western, R.A. Vertessy, A review of paired catchment studies for determining changes in water yield resulting from alterations in vegetation, J. Hydrol. 310 (1–4) (2005) 28–61, https://doi.org/10.1016/j.jhydrol.2004.12.010.

[16] P.N.J. Lane, A.E. Best, K. Hickel, L. Zhang, The response of flow duration curves to afforestation, J. Hydrol. 310 (1–4) (2005) 253–265, https://doi.org/10.1016/j.jhydrol.2005.01.006.

[17] D. Legesse, C. Vallet-Coulomb, F. Gasse, Hydrological response of a catchment to climate and land use changes in Tropical Africa: case study south central Ethiopia, J. Hydrol. 275 (1–2) (2003) 67–85, https://doi.org/10.1016/S0022-1694(03)00019-2.

[18] H.J. Chu, Y.P. Lin, C.W. Huang, C.Y. Hsu, H.Y. Chen, Modelling the hydrologic effects of dynamic land-use change using a distributed hydrologic model and a spatial land-use allocation model, Hydrol. Process. 24 (18) (2010) 2538–2554, https://doi.org/10.1002/hyp.7667.

[19] H. Moradkhani, R.G. Baird, S.A. Wherry, Assessment of climate change impact on floodplain and hydrologic ecotones, J. Hydrol. 395 (3–4) (2010) 264–278, https://doi.org/10.1016/j.jhydrol.2010.10.038.

[20] M.L. Warburton, R.E. Schulze, G.P.W. Jewitt, Confirmation of ACRU model results for applications in land use and climate change studies, Hydrol. Earth Syst. Sci. 14 (12) (2010) 2399–2414, https://doi.org/10.5194/hess-14-2399-2010.

[21] S.N. Gosling, R.G. Taylor, N.W. Arnell, M.C. Todd, A comparative analysis of projected impacts of climate change on river runoff from global and catchment-scale hydrological models, Hydrol. Earth Syst. Sci. 15 (1) (2011) 279–294, https://doi.org/10.5194/hess-15-279-2011.

[22] S.T.Y. Tong, Y. Sun, T. Ranatunga, J. He, Y.J. Yang, Predicting plausible impacts of sets of climate and land use change scenarios on water resources, Appl. Geogr. 32 (2) (2012) 477–489, https://doi.org/10.1016/j.apgeog.2011.06.014.

[23] Z. Li, W. zhao Liu, X. chang Zhang, F. li Zheng, Impacts of land use change and climate variability on hydrology in an agricultural catchment on the Loess Plateau of China, J. Hydrol. 377 (1–2) (2009) 35–42, https://doi.org/10.1016/j.jhydrol.2009.08.007.

[24] M.S. Aduah, G.P.W. Jewitt, M.L.W. Toucher, Assessing impacts of land use changes on the hydrology of a lowland rainforest catchment in Ghana, West Africa," Water (Switzerland) 10 (2017) 1, https://doi.org/10.3390/w10010009.

[25] T.J. Baker, S.N. Miller, Using the Soil and Water Assessment Tool (SWAT) to assess land use impact on water resources in an East African watershed, J. Hydrol. 486 (2013) 100–111, https://doi.org/10.1016/j.jhydrol.2013.01.041.

[26] K. Kuroda, et al., Recharge des eaux souterraines dans des régions suburbaines de Hanoï, Vietnam: effet de la diminution des niveaux des masses d'eaux de surface et des changements d'occupation du sol, Hydrogeol. J. 25 (3) (2017) 727–742, https://doi.org/10.1007/s10040-016-1528-2.

[27] H.P.A. Eweg, R. Van Lammeren, H. Deurloo, Z. Woldu, Analysing degradation and rehabilitation for sustainable land management in the highlands of Ethiopia, Land Degrad. Dev. 9 (6) (1998) 529–542, https://doi.org/10.1002/(SICI)1099-145X(199811/12)9:6<529::AID-LDR313>3.0. CO;2-O.

[28] M.E. Assessment, Ecosystems and Human Well-Being: Wetlands and Water, World Resources Institute, 2005.

[29] T. Gashaw, T. Tulu, M. Argaw, A.W. Worqlul, Modeling the hydrological impacts of land use/land cover changes in the Andassa watershed, Blue Nile Basin, Ethiopia, Sci. Total Environ. 619 (620) (2018) 1394–1408, https://doi.org/10.1016/j.scitotenv.2017.11.191.

[30] G. Muriuki, L. Seabrook, C. McAlpine, C. Jacobson, B. Price, G. Baxter, Land cover change under unplanned human settlements: a study of the Chyulu Hills squatters, Kenya, Landsc. Urban Plann. 99 (2) (2011) 154–165, https://doi.org/10.1016/j.landurbplan.2010.10.002.

[31] A.W. Yohannes, M. Cotter, G. Kelboro, W. Dessalegn, Land use and land cover changes and their effects on the landscape of Abaya-Chamo basin, Southern Ethiopia, Land 7 (2018) 1, https://doi.org/10.3390/land7010002.

[32] C. Mazengarb, I.G. Speden, Geology of the," *raukumara area, Geol. Map*, 2500001sheet+60pp, 6scale 14 (2000).

[33] G.L. Hargreaves, G.H. Hargreaves, J.P. Riley, Agricultural benefits for Senegal river basin, J. Irrigat. Drain. Eng. 111 (2) (1985) 113–124, https://doi.org/10.1061/(asce)0733-9437, 1985)111:2(113.

[34] Dereje Ayalew, Variability of rainfall and its current trend in Amhara region, Ethiopia, African J. Agric. Reseearch 7 (10) (2012), https://doi.org/10.5897/ajar11.698.

[35] Maurice G. Kendall, Kendall - Rank Correlation Methods-Griffin, 1970).pdf.", London, 1970.

[36] H.B. Mann, Non-Parametric Test Against Trend," Econometrica 13 (3) (1945) 245–259 [Online]. Available: http://www.economist.com/node/18330371?story%7B_%7Did=18330371.

[37] S. Addisu, Y.G. Selassie, G. Fissha, B. Gedif, Time series trend analysis of temperature and rainfall in lake Tana Sub-basin, Ethiopia, Environ. Syst. Res. 4 (1) (2015), https://doi.org/10.1186/s40068-015-0051-0.

[38] I. Larbi, F.C.C. Hountondji, T. Annor, W.A. Agyare, J.M. Gathenya, J. Amuzu, Spatio-temporal trend analysis of rainfall and temperature extremes in the Vea catchment, Ghana, Climate 6 (4) (2018) 1–17, https://doi.org/10.3390/cli6040087.

[39] R. Ali, A. Kuriqi, S. Abubaker, O. Kisi, Long-term trends and seasonality detection of the observed flow in Yangtze River using Mann-Kendall and Sen's innovative trend method, Water (Switzerland) 11 (2019) 9, https://doi.org/10.3390/w11091855.

[40] T. Pohlert, trend, Non-Parametric Trend Tests and Change-Point Detection (2020) 1–18 [Online]. Available: https://cran.r-project.org/package=trend%0Ahttps://orcid.org/0000-0003-3855-3025%0Afile:///C:/Users/staff/Documents/WSU/CentralUniversityofTechnology/CENTRALUNIVERSITY/MasterofCivilEngineering/MyThesis/Literature/ARIMA/Newfolder(2)/Pohlert2020.

[41] G.C. Okafor, O.D. Jimoh, K.I. Larbi, Detecting changes in hydro-climatic variables during the last four decades (1975-2014) on downstream kaduna river catchment, Nigeria, Atmos. Clim. Sci. 7 (2) (2017) 161–175, https://doi.org/10.4236/acs.2017.72012.

[42] L. Zhang, Z. Nan, Y. Xu, S. Li, Hydrological impacts of land use change and climate variability in the headwater region of the Heihe River Basin, northwest China, PLoS One 11 (6) (2016) 1–25, https://doi.org/10.1371/journal.pone.0158394.

[43] S.K. Jalota, B.B. Vashisht, S. Sharma, S. Kaur, Climate Change Projections, 2018, https://doi.org/10.1016/b978-0-12-809520-1.00002-1.

[44] C. Xu, From GCMs to river flow: a review of downscaling methods and hydrologic modelling approaches, Prog. Phys. Geogr. Earth Environ. 23 (2) (1999) 229–249, https://doi.org/10.1177/030913339902300204.

[45] T. Jiang, Y.D. Chen, C. yu Xu, X. Chen, X. Chen, V.P. Singh, Comparison of hydrological impacts of climate change simulated by six hydrological models in the Dongjiang Basin, South China, J. Hydrol. 336 (3–4) (2007) 316–333, https://doi.org/10.1016/j.jhydrol.2007.01.010.

[46] O. Batelaan, Zhong-Min Wang, F. De Smedt, An adaptive GIS toolbox for hydrological modelling, 1996, no, Appl. Geogr. Inf. Syst. Hydrol. water Resour. Manag. Proc. HydroGIS'96 Conf. Vienna 235 (1996) 3–9.

[47] Z.M. Wang, O. Batelaan, F. De Smedt, A distributed model for water and energy transfer between soil, plants and atmosphere (WetSpa), 3 SPEC. ISS, Phys. Chem. Earth 21 (1996) 189–193, https://doi.org/10.1016/S0079-1946(97)85583-8.

[48] O. Batelaan, F. De Smedt, GIS-based recharge estimation by coupling surface-subsurface water balances, J. Hydrol. 337 (3–4) (2007) 337–355, https://doi.org/10.1016/j.jhydrol.2007.02.001.

[49] S.T. Woldeamlak, O. Batelaan, F. De Smedt, Effects of climate change on the groundwater system in the Grote-Nete catchment, Belgium, Hydrogeol. J. 15 (5) (2007) 891–901, https://doi.org/10.1007/s10040-006-0145-x.

[50] R.G. Allen, L.S. Pereira, D. Raes, M. Smith, FAO Irrigation and Drainage Paper No. 56 - Crop Evapotranspiration, 1998 no. January 1998.

[51] J. R. W. S.L. NEITSCH, J.G. Arnold, J.R. Kiniry, S Oil and W Ater a Ssessment T Ool D Ocumentation, 2005.

[52] K.J. Lim, B.A. Engel, Z. Tang, J. Choi, Automated_Web_GIS_based_Hydrograph_Analysis_Tool_WHAT_JAWRA_Dec_2005, WHAT. J. Am. Water Resour. Assoc. 1397 (6) (2005) 1407–1416 [Online]. Available: https://engineering.purdue.edu/mapserve/WHAT/faq/Automated_Web_GIS_based_Hydrograph_Analysis_Tool_WHAT_JAWRA_Dec_2005.pdf.

[53] C. I. Voss and A. Provost, "Version of September 22, 2010 (SUTRA Version 2.2) Latest version available at: ,http://water.usgs.gov/nrp/gwsoftware" *USGS Water Resour. Investig. Rep*p. 02–*4231*, vol. 2010, 2010, [Online]. Available: http://pysot.readthedocs.io/en/latest/index.html.

[54] Lyne, January 1979, Hollick, "Stochastic Time-Variable Rainfall-Runoff Modeling (1979).

[55] K. Eckhardt, How to construct recursive digital filters for baseflow separation, Hydrol. Process. 19 (2) (2005) 507–515, https://doi.org/10.1002/hyp.5675.

[56] L. Kumar, Climate Change and Impacts in the Pacific, 2020.

[57] D. Reay, C. Sabine, P. Smith, G. Hymus, Intergovernmental Panel on climate change. Fourth assessment report, Available from, in: Inter-gov- Ernmental Panel on Climate Change, Cambridge; UK: Cambridge University Press, Geneva, Switzerland, 2007. : 2007. doi: 10.1038/446727a.

[58] T. Shah, Climate change and groundwater: India's opportunities for mitigation and adaptation, Environ. Res. Lett. 4 (3) (2009), https://doi.org/10.1088/1748-9326/4/3/035005.

[59] C.P. Kumar, G.J. Chakrapani, Climate change and its influence on groundwater resources, Curr. Sci. 105 (1) (2012) 37–46.

[60] A.A. Gessesse, A.M. Melesse, F.F. Abera, A.Z. Abiy, Modeling hydrological responses to land use dynamics, Choke, Ethiopia, Water Conserv. Sci. Eng. 4 (4) (2019) 201–212, https://doi.org/10.1007/s41101-019-00076-3.

[61] T. Getu Engida, T. A. Nigussie, A. B. Aneseyee, and J. Barnabas, "Land use/land cover change impact on hydrological process in the upper baro basin, Ethiopia," Appl. Environ. Soil Sci., vol. 2021, 2021, doi: 10.1155/2021/6617541.

[62] A. Birhanu, I. Masih, P. van der Zaag, J. Nyssen, X. Cai, Impacts of land use and land cover changes on hydrology of the Gumara catchment, Ethiopia, Phys. Chem. Earth 112 (2019) 165–174, https://doi.org/10.1016/j.pce.2019.01.006.

[63] S. Tekleab, Y. Mohamed, S. Uhlenbrook, J. Wenninger, Hydrologic responses to land cover change: the case of Jedeb mesoscale catchment, Abay/Upper Blue Nile Basin, Ethiopia, Hydrol. Process. 28 (20) (2014) 5149–5161, https://doi.org/10.1002/hyp.9998.

[64] T.D. Mengistu, I.M. Chung, M.G. Kim, S.W. Chang, J.E. Lee, Impacts and implications of land use land cover dynamics on groundwater recharge and surface runoff in East African watershed, Water (Switzerland) 14 (2022) 13, https://doi.org/10.3390/w14132068.

[65] F. Warku, T. Korme, G. Kabite, D. Nedow, Impacts of land use/cover change and climate variability on groundwater recharge for upper Gibe watershed , Ethiopia, Sustain. Water Resour. Manag. 8 (1) (2022) 1–16, https://doi.org/10.1007/s40899-021-00588-8.

[66] J. Sun, et al., Effects of forest structure on hydrological processes in China, J. Hydrol. 561 (March) (2018) 187–199, https://doi.org/10.1016/j.jhydrol.2018.04.003.

[67] G. Wang, J. Li, W. Sun, B. Xue, , Y, A, T. Liu, Non-point source pollution risks in a drinking water protection zone based on remote sensing data embedded within a nutrient budget model, Water Res. 157 (2019) 238–246, https://doi.org/10.1016/j.watres.2019.03.070.

[68] T.A. Ansari, Y.B. Katpatal, A.D. Vasudeo, Spatial evaluation of impacts of increase in impervious surface area on SCS-CN and runoff in Nagpur urban watersheds, India, Arabian J. Geosci. 9 (2016) 18, https://doi.org/10.1007/s12517-016-2702-5.

[69] J.E. Vogelmann, A.L. Gallant, H. Shi, Z. Zhu, Perspectives on monitoring gradual change across the continuity of Landsat sensors using time-series data, Remote Sens. Environ. 185 (2016) 258–270, https://doi.org/10.1016/j.rse.2016.02.060.

[70] S.L. Gebre, Potential impacts of climate change on the hydrology and water resources availability of Didessa catchment, Blue nile river basin, Ethiopia, J. Geol. Geosci. 4 (1) (2015) 1–7, https://doi.org/10.4172/2329-6755.1000193.

[71] A.T. Haile, A.L. Akawka, B. Berhanu, T. Rientjes, Changes in water availability in the Upper Blue Nile basin under the representative concentration pathways scenario, Hydrol. Sci. J. 62 (13) (2017) 2139–2149, https://doi.org/10.1080/02626667.2017.1365149.

[72] H.G. Rendilicha, A review of groundwater vulnerability assessment in Kenya, Acque Sotterranee - Italian Journal of Groundwater 7 (2) (2018), https://doi.org/10.7343/as-2018-328.

[73] A. Ertürk, A. Ekdal, M. Gürel, N. Karakaya, C. Guzel, E. Gönenç, Evaluating the impact of climate change on groundwater resources in a small Mediterranean watershed, Sci. Total Environ. 499 (2014 Nov 15) 437–447, https://doi.org/10.1016/j.scitotenv.2014.07.001. Epub 2014 Jul 23. PMID: 25064798.

[74] G.F. Boru, Z.B. Gonfa, G.M. Diga, Impacts of climate change on stream flow and water availability in Anger sub-basin, Nile Basin of Ethiopia, Sustain. Water Resour. Manag. 5 (2019) 1755–1764, https://doi.org/10.1007/s40899-019-00327-0.